

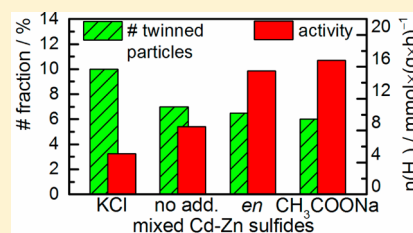
On the Formation of Cd–Zn Sulfide Photocatalysts from Insoluble Hydroxide Precursors

Anton Litke, Jan P. Hofmann, Thomas Weber, and Emiel J. M. Hensen*

Inorganic Materials Chemistry Group, Department of Chemical Engineering and Chemistry, Eindhoven University of Technology, P.O. Box 513, 5600 MB, Eindhoven, The Netherlands

Supporting Information

ABSTRACT: The formation of Cd–Zn sulfide solid solutions from mixed hydroxides under hydrothermal conditions is investigated in detail. The work specifically aims to understand the formation and the role of nanotwinned mixed sulfide particles that have been reported to show excellent performance in photocatalytic water splitting (Liu, M.; et al. *Energy Environ. Sci.* **2011**, *4*, 1372). The influence of additives, pH, autoclave tumbling, and the state of the mixed hydroxide precursor on the mixed sulfides was studied by XRD, XPS, TEM, DR UV–vis, and N₂ physisorption. Cd–Zn sulfides are formed via a dissolution–precipitation mechanism. Agitation of the synthetic medium and the formation of soluble intermediate complexes during hydrothermal treatment suppress the formation of a hexagonal wurtzite crystal phase and improve the photocatalytic activity of the mixed sulfides. The role of additives can be understood in terms of complex formation, pH maintenance, and adsorption on the facets of growing crystallites. All Cd–Zn sulfide samples exhibit compositional inhomogeneities, resulting in XRD line broadening and decreased bandgaps as compared with the values predicted by Vegard's law. Detailed TEM analysis revealed that the samples with higher amounts of nanotwinned particles were significantly less active in water reduction. The influence of nanotwinned particles is discussed in terms of extended crystal defects and charge carrier recombination.



INTRODUCTION

Growing energy demand and finite reserves of fossil fuels, which make up 80% of the global energy supply nowadays, challenge our society to move toward renewable energy sources.¹ Among renewable energy sources, solar energy is considered as one of the most promising options, because the amount of energy that our planet receives in the form of solar radiation surpasses our current and projected future demands by several orders of magnitude. A key challenge of solar energy harvesting is its intermittency. One possible solution is to store the energy of the photons in chemicals. Direct conversion of solar radiation into energy-dense fuels can be achieved by means of photocatalytic water splitting. Various photocatalytic systems based on metal oxides, nitrides, chalcogenides, and other inorganic semiconductors have been developed since the 1970s.² Unfortunately, many of these materials are active only under UV irradiation (e.g., TiO₂, ZnO, SrTiO₃) or contain scarce and expensive materials (e.g., GaAs, InP, CuIn_{1-x}Ga_xS₂).^{3–5} Another factor, which hinders large-scale implementation of this technology, is the low energy conversion efficiency of most photocatalysts.² The efficiency depends on parameters such as the bandgap, charge carrier mobility, and kinetics of the surface redox reactions. In this sense, metal chalcogenides are considered a promising class of materials for photocatalytic water reduction, because they can be synthesized by means of facile techniques, and different strategies can be implemented to adjust their properties and optimize performance.⁶ For instance, the bandgap of transition

metal chalcogenides can be adjusted to a wide range by doping with other chalcogenides or metals.^{7,8} Some metal sulfides (e.g., WS₂, MoS₂) have been successfully combined with other chalcogenides as cocatalysts for water reduction in place of noble metals.⁹ A drawback is that a hole scavenger is usually needed to avert the negative effect which photocorrosion has on their stability.

Among chalcogenides, mixed cadmium–zinc sulfides are one of the most extensively studied systems. These sulfides can be prepared with different metal ratios, particle sizes, and morphologies using various synthetic methods.^{9–11} A particularly active system based on this material has been recently reported by Liu et al.¹⁰ In this work, an insoluble mixed Cd–Zn hydroxide was used as a precursor in a hydrothermal synthesis of mixed sulfides. The authors ascribed the high photocatalytic activity of their samples to the presence of nanotwinned particles. These particles contain regions of the crystal structure “mirrored” against twin planes. Liu et al. proposed that there is an electrical field at a twin plane, which drastically improves charge carrier separation and boosts up overall photocatalytic performance of the material.^{10,12} However, to the best of our knowledge, there are no published studies, which scrutinize this approach that involves insoluble mixed hydroxide as a metal precursor. In addition, quantification of the correlation between

Received: June 22, 2015

Published: September 17, 2015

nanotwinned particles and photocatalytic activity¹⁰ is still missing.

To optimize the performance of the Cd–Zn sulfides, it is useful to understand the mechanism of their formation so that the influence of parameters, such as polarity of the solvent, ionic strength and composition of the medium, and the presence of capping agents, can be better predicted. The use of insoluble hydroxides as starting chemicals in the synthesis of mixed sulfides requires knowledge about their composition, crystallinity, and thermal stability to predict their behavior during hydrothermal synthesis. It is unclear how the nanotwinned particles form and whether their yield can be controlled. The influence of the nanotwinned particles on the photocatalytic activity of Cd–Zn sulfides may be difficult to ascertain, because these particles contain numerous extended defects of the crystal structure (i.e., twins, stacking faults, and dislocations) and the activity of a photocatalyst strongly depends on its crystallinity.^{13,14} For instance, surface defects of TiO₂ particles can trap charge carriers and enhance photocatalytic activity, while bulk defects act as recombination centers compromising activity.¹⁵

In this work, we investigated the formation of mixed Cd–Zn sulfides and how synthesis parameters, such as tumbling, organic and inorganic additives, and ionic strength of the reaction medium, influence the photocatalytic activity of the final sulfide products. Insoluble mixed Cd–Zn hydroxide and thioacetamide were used as metal and sulfur precursor, respectively. We found that additives, which induce formation of Zn and Cd complexes, suppress formation of nanotwinned particles and enhance photocatalytic activity. On the basis of the experimental results, an overall mechanism of the transformation of the insoluble mixed hydroxide precursor into the mixed sulfide is proposed.

■ EXPERIMENTAL SECTION

Mixed Cd–Zn sulfides were prepared from insoluble mixed Cd–Zn hydroxides unless otherwise stated. We used a single batch of dry Cd–Zn hydroxide to avoid deviation of the metal composition among different syntheses. We prepared one sample from freshly precipitated mixed hydroxide to evaluate whether the water content of the hydroxide had any influence on the properties of the final material. Samples of ZnS and CdS were synthesized from the corresponding freshly precipitated hydroxides. One sample of Cd_{0.5}Zn_{0.5}S was prepared by coprecipitation with Na₂S as a reference for the comparison of the photocatalytic activity with the reported values.¹⁰

Chemicals. Cd(NO₃)₂·4H₂O (Sigma-Aldrich, ≥99%), Zn(NO₃)₂·6H₂O (Sigma-Aldrich, ≥98%), NaOH (Sigma-Aldrich, ≥98%), Cd(CH₃COO)₂·4H₂O (Sigma-Aldrich, ≥98%), Zn(CH₃COO)₂·2H₂O (Sigma-Aldrich, ≥98%), thioacetamide (Sigma-Aldrich, >99%), Na₂SO₄ (Sigma-Aldrich, ≥99%), 1,2-ethylenediamine (Sigma-Aldrich, ≥99%), 1,3-propanediamine (Sigma-Aldrich, ≥99%), HCOONa (Sigma-Aldrich, ≥99%), CH₃COONa (Sigma-Aldrich, ≥99%), C₂H₅COONa (Alfa Aesar, 99%), Na₂S·9H₂O (Sigma-Aldrich, ≥98%), Na₂SO₃ (Sigma-Aldrich, 98–100%), and ethanol absolute (VWR, technical grade) were used as received without further purification. In all experiments, demineralized water (resistivity >15 MΩ·cm at 25 °C) was used for the preparation of solutions and washing of the solid samples.

Preparation of Dry Mixed Cd–Zn Hydroxide. A batch of mixed cadmium–zinc hydroxide with 1:1 metal ratio was prepared by coprecipitation from an aqueous solution of Zn(NO₃)₂ and Cd(NO₃)₂ with NaOH: 200 mL of 4 M NaOH solution was added dropwise under magnetic stirring into a 1000 mL round-bottom flask containing 300 mL of a solution of Zn²⁺ and Cd²⁺ nitrates (0.1 mol of each salt). Alkaline addition was continued until visible precipitation stopped and the pH of the solution reached 12. The suspension of the mixed

hydroxide was stirred for 30 min and then separated on a Büchner funnel, and washed twice with demineralized water and once with absolute ethanol. The white solid product was dried in a vacuum oven at 50 °C until the mass did not change anymore. The dry Cd–Zn hydroxide was ground, transferred into an airtight glass jar, and used as the precursor for the synthesis of mixed sulfide.

Synthesis of Mixed Cd–Zn Sulfide from Dry Hydroxide. Unless otherwise stated, samples of mixed Cd–Zn sulfide were prepared from mixed hydroxide using the following procedure. A 0.92 g ($n(\text{Cd} + \text{Zn}) \approx 7 \times 10^{-3}$ mol) portion of dry mixed hydroxide was dispersed for 15 min under magnetic stirring in 35 mL of demineralized water. Then 7.7×10^{-3} mol thioacetamide was added to the dispersion, and the mixture was stirred for 10 min. Afterward, the mixture was transferred into a PTFE-lined stainless steel autoclave (45 mL capacity), sealed, and heated at 180 °C for 24 h under tumbling. After the hydrothermal treatment, the autoclave was rapidly cooled to room temperature. The insoluble yellow product was separated from the mother solution by means of centrifugation, and washed twice with demineralized water and once with absolute ethanol. The resulting solid was dried under vacuum at room temperature, ground, weighed, and used for further characterization and tests.

Preparation of samples in the presence of additives is identical to the method described above except that an aqueous solution of the respective additive was used instead of demineralized water. The following additive concentrations were used: 0.1 M, 1.0 M, 1.5 M CH₃COONa; 0.1 and 1.0 M HCOONa, C₂H₅COONa, KCl, or Na₂SO₄; 0.1 M, 0.2 M, 0.5 M 1,2-ethylenediamine (en); 0.1 and 0.2 M 1,3-propylenediamine (pn), and 0.1 M NaOH.

Synthesis of Mixed Cd–Zn Sulfides from Freshly Precipitated Mixed Hydroxide. A 50 mL portion of an aqueous solution containing 2×10^{-3} mol NaOH was added dropwise under stirring into 50 mL of a solution containing Zn(NO₃)₂ and Cd(NO₃)₂ (5×10^{-3} mol of each). The white precipitate was separated from the supernatant, washed twice with demineralized water, and dispersed in 35 mL of an 1.0 M CH₃COONa aqueous solution. Then 1.1×10^{-3} mol of thioacetamide was added, and the mixture was stirred for 10 min before being transferred into a PTFE-lined stainless steel autoclave and subjected to the hydrothermal treatment. The synthesis conditions and the product collection were identical to those described in the previous section.

Synthesis of ZnS and CdS from Insoluble Pure Hydroxides. Samples of ZnS and CdS were synthesized from freshly precipitated Zn(OH)₂ and Cd(OH)₂, respectively. First, the insoluble hydroxides were obtained by adding 20 mL of 1.0 M NaOH into 50 mL of an aqueous solution containing 1×10^{-3} mol zinc or cadmium nitrate. The alkali was added dropwise under vigorous stirring. The precipitate was separated by means of centrifugation and washed twice with deionized water. Then the insoluble hydroxide was dispersed in 35 mL of an 1.0 M sodium acetate aqueous solution, or demineralized water. After that, 1.1×10^{-3} mol of thioacetamide was added into the dispersion. The mixture was left for 10 min under magnetic stirring and underwent the hydrothermal treatment and product collection as described for mixed Cd–Zn sulfide.

Synthesis of Zn_{0.5}Cd_{0.5}S by Coprecipitation. A reference sample was prepared by coprecipitation from a zinc and cadmium acetate mixed solution (40 mL, 1×10^{-3} mol of each metal) with sodium sulfide (40 mL, 1.1×10^{-3} mol Na₂S). The precipitate was separated by means of centrifugation, washed twice with demineralized water and once with ethanol, and dried under vacuum at room temperature.

Characterization. The morphology of the particles was characterized by means of bright-field transmission electron microscopy using FEI Technai G2 (type Sphera) instrument equipped with a LaB₆ source and operated at 200 kV. XRD patterns were collected on a Bragg–Brentano Bruker Endeavor D2 powder diffractometer equipped with a Cu cathode and a 1D LYNXEYE detector (Ni-filtered K β , 1.0 mm primary beam slit and 3.0 mm beam knife height). XPS spectra were recorded on a Thermo K-Alpha spectrometer equipped with a monochromated Al K α X-ray source (spectral

resolution 0.1 eV, dwell time 50 ms, averaging of 10 scans). Diffuse-reflectance UV–vis spectra were obtained on a Shimadzu UV-2401PC UV–vis spectrometer equipped with an integrated sphere, using BaSO₄ as a reference material. The BET surface area was determined from N₂ physisorption isotherms collected on an ASAP Tristar II module. Thermogravimetric analysis was performed on a DSC 1 module (Mettler Toledo) in the range 50–700 °C employing a heating rate of 10 °C/min. Data processing is detailed in the Supporting Information.

Photocatalytic Activity Measurements. All photocatalytic tests were carried out in a home-built gaseight photocatalytic setup in a side-illuminated PEEK cell. The amount of produced H₂ was detected with an online GC-TCD (ShinCarbon column, N₂ as a carrier gas). A 500 W Hg(Xe) lamp was used as the light source. The IR and UV components of the emission spectrum were removed by means of demineralized water and a 420 nm cutoff glass filter (OD⁴¹⁰ = 5.0). A light intensity controller (model 68950, Newport) was used to maintain a constant light flux in the experiments. In this way, the amount of the produced hydrogen was determined as a function of time. The hydrogen production rate was used to compare the photocatalytic activities of the samples.

In a typical test, we used 10 mg of a photocatalyst. The solid was dispersed under sonication in 10 mL of a solution containing sacrificial agents (0.25 M Na₂S and 0.35 M Na₂SO₃). Then, the dispersion was transferred into the PEEK cell and diluted with the sacrificial reagent solution to 50 mL. The photocatalyst loading was always 0.2 g/L. Before each test, dissolved air was removed by evacuation. The activity measurements were carried out under constant stirring with automated sampling of the gaseous products at 12 min intervals. The temperature of the solution was maintained at 20 °C.

Photoplatinization of Mixed Cd–Zn Sulfides. Photodeposition of Pt on mixed Cd–Zn sulfides was carried out in the same equipment as used for the photocatalytic activity measurements. An amount of 57 μL of H₂PtCl₆ solution (0.87 mg_{Pt}/mL) was added to a dispersion of 10 mg of mixed Cd–Zn sulfides in 50 mL of sacrificial solution (0.25 M Na₂S and 0.35 M Na₂SO₃). After evacuation, the mixture was illuminated by visible light (λ > 420 nm) under constant stirring. Gaseous products were sampled at 4 min intervals. Hydrogen evolution rates of three consecutive runs (the head space was evacuated in between runs) were averaged to estimate photocatalytic activity of platinumized samples.

Elemental Analysis. The metal composition of mixed Cd–Zn hydroxide and sulfides was measured by means of inductively coupled plasma atomic emission spectroscopy on a SPECTRO BLUE ICP-OES instrument. Solid samples were dissolved in nitric acid (99.999% metal basis) for analysis. Calibration of the instrument was carried out with Zn and Cd standard solutions, and the samples were measured in duplicate.

RESULTS AND DISCUSSION

Composition of the Mixed Hydroxide Precursor. In order to understand the transformation of insoluble mixed Cd–Zn hydroxide under hydrothermal conditions and its role in the synthesis of mixed sulfides, we studied its crystal phase composition and thermal stability. The XRD pattern of the dry mixed hydroxide is shown in the Figure 1. Reflections in the diffractogram can be assigned to trigonal Cd(OH)₂, while the broad feature in the 15–45° 2θ region is related to the formation of amorphous Zn(OH)₂.¹⁶ Cd(OH)₂ reflections did not shift compared with those of pure Cd(OH)₂. Thus, we can conclude that no solid solution of Zn in Cd(OH)₂ was formed in the hydroxide precursor, but rather a physical mixture of crystalline Cd(OH)₂ and amorphous Zn(OH)₂ was formed. The formation of two separate hydroxides was further confirmed by TGA as we observed stepwise decomposition of Zn(OH)₂ and Cd(OH)₂ to the corresponding oxides (Figure S1, Supporting Information).

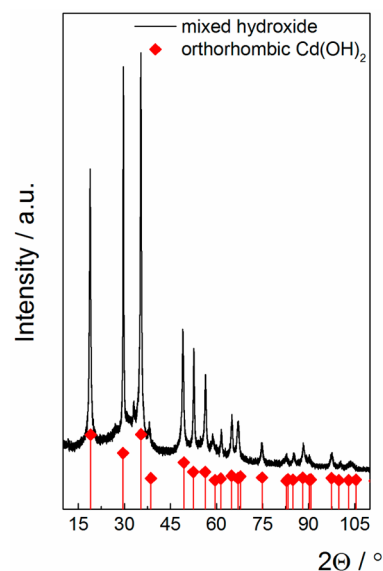


Figure 1. XRD pattern of the mixed Cd–Zn hydroxide and a reference pattern of orthorhombic Cd(OH)₂ (PDF 01-073-6989).

Influence of Mechanical Agitation and Additives on the Photocatalytic Activity of Mixed Cd–Zn Sulfides.

We first studied the influence of mechanical agitation of the synthesis solution and the presence of additives on the photocatalytic properties of the resulting mixed sulfides. In the reference work, the insoluble hydroxide was not separated from the supernatant, so that the final solution contained a substantial amount of sodium acetate (about 0.8 M).¹⁰ To investigate how the presence of sodium acetate and tumbling influences the photocatalytic properties of the resulting mixed sulfides, we prepared two samples in 1.0 M CH₃COONa: one in a tumbled and the other in a static autoclave, and one sample in demineralized water under tumbling. XRD patterns, surface areas, bandgaps, and photocatalytic activities of these samples are reported in Figure 2. Comparison of experimental XRD patterns with the reference peak positions reveals that solid solutions of Cd–Zn sulfide were formed in all cases. The crystal phase of the samples prepared in a tumbled autoclave can be assigned as cubic, while the sample prepared in a static

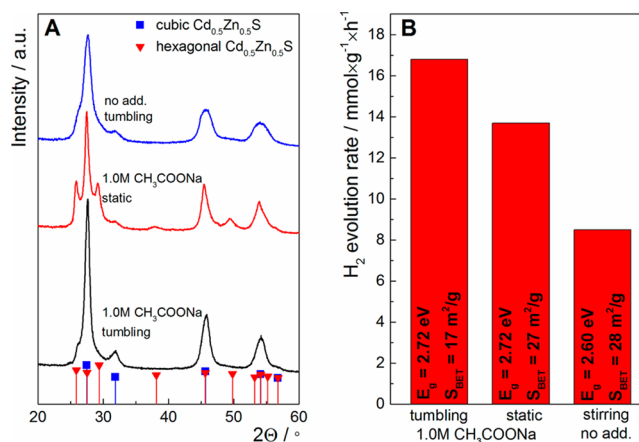


Figure 2. Cd–Zn sulfides prepared in demineralized water (i.e., no additives) or 1.0 M CH₃COONa in a tumbled or in a static autoclave: (A) XRD patterns; (B) hydrogen evolution rates, bandgaps, and BET surface areas.

autoclave contained a substantial amount of the hexagonal phase (wurtzite) along with the cubic zinc blende phase. The XRD lines of the sample prepared in demineralized water were broader than those of the samples prepared in 1.0 M CH_3COONa . The diffractograms contained no reflections due to impurity phases (e.g., ZnO or $\text{Cd}(\text{OH})_2$) indicating complete conversion of the insoluble hydroxide into a sulfide phase (Figure 2A).

Samples prepared in 1.0 M CH_3COONa were substantially more active than sulfides prepared in demineralized water (Figure 2B). This means that the presence of sodium acetate in the synthesis medium influences the photocatalytic activity of $\text{Cd}_{0.5}\text{Zn}_{0.5}\text{S}$. Mechanical agitation of the synthesis mixture suppressed formation of the hexagonal crystal phase and had a positive effect on the photocatalytic activity (Figure 2B). It is known from literature that CdS forms the hexagonal phase at low chemical potential of S^{2-} whereas the cubic phase is formed at high S^{2-} potential.¹⁷ Thus, when the mixture is not agitated, insoluble hydroxide that settled at the bottom of the static autoclave will form the hexagonal phase due to mass transport limitations of the sulfur species.

We found that the influence of sodium acetate on the photocatalytic activity of the mixed sulfide was concentration dependent. The samples prepared in 0.1, 1.0, and 1.5 M CH_3COONa were about 1.3, 2.0, and 2.1 times more active than the sulfide prepared in demineralized water, while the surface areas, XRD patterns, and bandgaps of the samples were comparable (Figure S2, Supporting Information). This means that the difference in photocatalytic activity relates to properties of the material (crystal defects, trapping states, charge carrier mobility, etc.), which cannot be probed by these bulk characterization techniques.

The discovered positive effect of sodium acetate on the photocatalytic activity of $\text{Cd}_{0.5}\text{Zn}_{0.5}\text{S}$ can in principle be the result of the specific chemical interaction of acetate with the reacting species or due to the change in the ionic strength of the reaction medium. To determine the possible role of the ionic strength, we synthesized Cd-Zn sulfide in 0.1 and 1.0 M Na_2SO_4 or KCl solutions. Chlorides and sulfates of zinc and cadmium are commonly used in the synthesis of mixed sulfides.^{18–21} When precipitation of the insoluble precursor and the hydrothermal treatment are carried out in the same vessel without removal of the salts as performed by Liu et al.,¹⁰ the resulting Na_2SO_4 or KCl can influence the properties of the material. For instance, there are publications indicating that the type of anion in precursors strongly influences photocatalytic activity of mixed sulfides.^{20,21}

The XRD patterns and photocatalytic activities of samples prepared in the presence of chloride or sulfate are shown in Figure 3. XRD reflections of these samples were typically sharper than those of the samples prepared in demineralized water. The main diffraction peaks of all sulfides can be assigned to the cubic $\text{Cd}_{0.5}\text{Zn}_{0.5}\text{S}$ phase. Samples prepared in KCl solution had shoulders next to the main peak and two weak reflections at 38 and 49° 2θ , indicating the formation of the hexagonal $\text{Cd}_{0.5}\text{Zn}_{0.5}\text{S}$ phase (Figure 3A). The photocatalytic activities of the samples prepared in the presence of chloride were the lowest (Figure 3B). This effect is unlikely to originate from the incorporation of KCl into the product, as neither potassium nor chloride was detected by means of XPS (see Supporting Information Figure S3). The main reason for the decreased activity could be the formation of the hexagonal phase, as in the case of the static autoclave (Figure 2). The

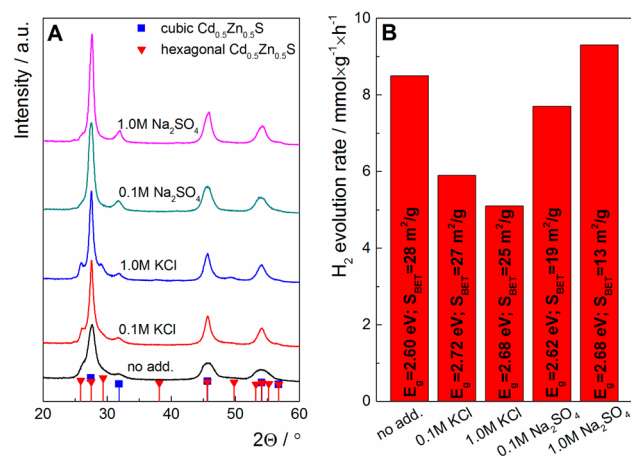


Figure 3. Cd-Zn sulfides prepared in a tumbled autoclave in 0.1 or 1.0 M aqueous solutions of KCl or Na_2SO_4 : (A) XRD patterns; (B) hydrogen evolution rates, bandgaps, and BET surface areas. The sample prepared in demineralized water (no additives) is included as a reference.

effect of sodium acetate cannot be assigned solely to the ionic strength of the reaction medium. Solutions with 0.1 M KCl and CH_3COONa have the same ionic strength (this also applies to the corresponding 1.0 M solutions), but these salts have an opposite effect on the photocatalytic activity (Figure 3B and Figure S2B). The ionic strength of the Na_2SO_4 solution is three times higher than the ionic strength of either KCl or CH_3COONa solutions of the same concentration; this difference has, however, negligible effect on the photocatalytic activity.

Thus, the role of sodium acetate is of chemical nature. Either, it acts as a surfactant related to the hydrophobic CH_3 or hydrophilic COO^- groups, or it maintains the relatively high pH of the medium throughout the hydrothermal treatment (Table S1, Supporting Information). To discriminate between these two effects we prepared mixed Cd-Zn sulfide in the presence of sodium formate, sodium acetate, and sodium propionate. The properties of the samples prepared in 1.0 M solutions of these carboxylates were very similar (Figure 4).

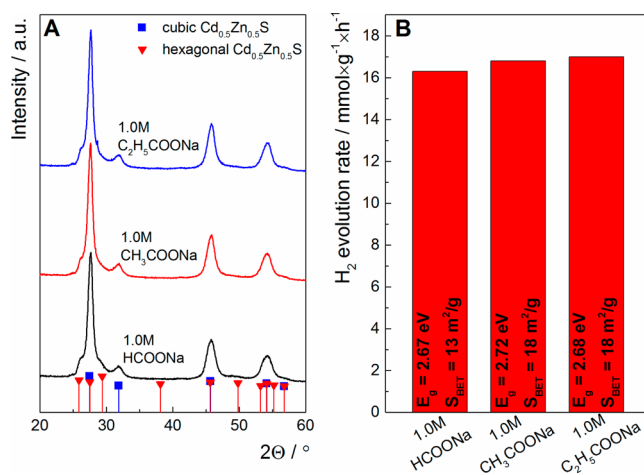


Figure 4. Cd-Zn sulfides prepared in a tumbled autoclave in 1.0 M solutions of sodium formate, acetate, and propionate: (A) XRD patterns; (B) hydrogen evolution rates, bandgaps, and BET surface areas.

The difference of the photocatalytic activity was within the experimental error, which has been estimated to be about 7%. Propionate and acetate at lower concentrations (0.1 M) affected the properties of the mixed sulfide in a similar manner as well (Supporting Information, Figure S4). These findings rule out a surfactant-related role, as these salts are expected to behave differently as surfactants. At the same time, they have similar pK_a values (Table S2, Supporting Information), which suggests that relatively high pH of the synthesis medium is important for the formation of highly active Cd–Zn sulfides from the mixed insoluble hydroxide.

High pH of the solution favors the formation of zinc and cadmium hydroxo-complexes (Table 1), which can act as

Table 1. Cumulative Formation Constants of Zn^{2+} and Cd^{2+} Complexes²²

	Zn^{2+}	Cd^{2+}
	OH [−] Ligand	
log K_1	4.4	5.77
log K_2	11.3	10.83
log K_3	14.14	14.11
log K_4	17.66	n.a.
	en Ligand	
log K_1	4.17	5.47
log K_2	8.33	10.09
log K_3	9.02	12.09
log K_4	8.67	n.a.

solution intermediates in the transformation of the insoluble hydroxide into the sulfide. However, we found that a highly basic medium (0.1 M NaOH) resulted in the formation of two separate Zn- or Cd-rich phases with no positive effect on the photocatalytic activity of the sample (Figure S5, Supporting Information). This can be explained by the fact that OH[−] coordinates much more strongly to Zn^{2+} than to Cd^{2+} , which will result in a substantial difference of the concentration of zinc and cadmium hydroxo-complexes in the solution at high pH. This difference may lead to the sequential precipitation of Zn- and Cd-rich sulfides, which in turn can explain why the moderate pH values of the 1.0 M sodium carboxylates solutions are preferred for the formation of the highly active mixed sulfide.

To prove the hypothesis that transition metal complexes are involved in the formation of active Cd–Zn sulfide we prepared several samples in the presence of ethylenediamine (en). Like OH[−], this ligand does form stronger complexes with Zn^{2+} than with Cd^{2+} (Table 1). Figure 5 shows the XRD patterns and the results of the photocatalytic tests of the samples prepared in 0.1, 0.2 and 0.5 M en. The effect of en on the photocatalytic activity is concentration dependent, and the most active sample was obtained at an en concentration of 0.2 M. We surmise that this optimum relates to the chelating properties of 1,2-ethylenediamine rather than to the high pH of the medium. First, when the en concentration was increased from 0.1 to 0.2 M, the activity increased by more than 20%, while this only led to a small change of the pH of the solution (Table S1). Second, we have shown before that a higher pH during synthesis does not have a positive effect on the activity (Figure S5, Supporting Information). Related to this, we found that an increase of the en concentration to 0.5 M had a detrimental effect on the activity of the samples because Zn- and Cd-rich phases formed (Figure 5). 1,3-Propylenediamine had similar effect on the

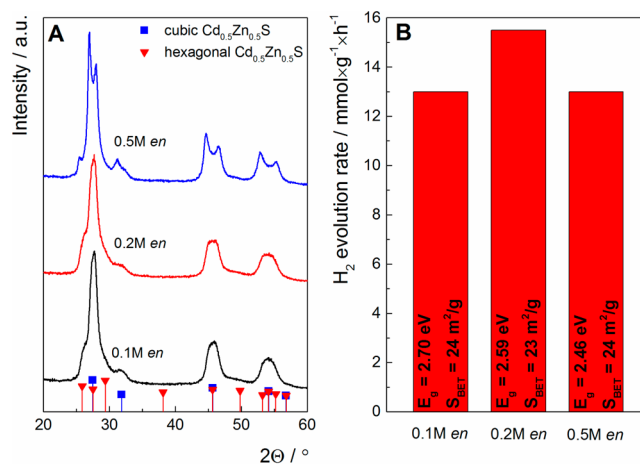


Figure 5. Cd–Zn sulfides prepared with tumbling in 0.1, 0.2, and 0.5 M en solutions: (A) XRD patterns; (B) hydrogen evolution rates, bandgaps, and BET surface areas.

photocatalytic activities of the mixed sulfides (Figure S6, Supporting Information).

In summary, we conclude that the formation of Zn^{2+} and Cd^{2+} complexes plays a central role in the synthesis of highly active mixed sulfides from the suspension of insoluble Zn and Cd hydroxides. From a comparison of the solubility products, one can establish that the conversion of the hydroxide into the sulfide is more favorable for Cd than for Zn (Table S3, Supporting Information). Thus, it is important to use ligands in the solution that form stronger complexes with Zn than with Cd: OH[−] and en are examples of such ligands. Their presence will result in higher concentration of Zn^{2+} species in the reaction medium and favor precipitation of the mixed sulfide.

As we suggested that soluble complexes of Zn^{2+} and Cd^{2+} are important intermediates in the conversion of the mixed insoluble hydroxides into the sulfide, we investigated whether additives like CH_3COONa have a similar effect on the formation of ZnS and CdS from the corresponding pure hydroxides. However, we found that the properties of ZnS and CdS prepared in demineralized water or in 1.0 M CH_3COONa were identical (Figure S7, Supporting Information). This means that the formation of metal complexes during synthesis has a synergetic effect only for the mixed system but not for the separate metal sulfides. It is consistent with our hypothesis that maintaining a particular ratio of soluble Zn and Cd intermediates throughout synthesis is important for the formation of the active mixed sulfide.

XRD Pattern Analysis: Compositional Deviation in the Solid Solution. One can see that the XRD reflections of all mixed sulfides were substantially broader than those of the pure ZnS and CdS materials. Such line broadening is often attributed to the small size of the coherently scattering domains²³ while other factors such as stresses in the crystal lattice, compositional inhomogeneities, and a large number of extended defects in the crystallites (i.e., twins, stacking faults, or dislocations) can also induce line broadening.^{24–26} To elucidate which factors account for line broadening in our samples, we carried out a detailed XRD pattern analysis, which is complemented by analysis of the particle size and the fraction of nanotwinned crystals observed in TEM images.

To determine the contribution of size and stress into line broadening, we used the Hall–Williamson plot²⁵ and Rietveld refinement.²⁷ Both methods yielded consistent results for ZnS

and CdS (Figures S8 and S9 in Supporting Information). The Williamson–Hall plot showed no prominent anisotropy of the strain distribution, which would manifest as a linear trend of the line broadening along a particular crystal orientation. The mean particle sizes extracted from the XRD data were smaller than those obtained from TEM analysis (Figure S10, Supporting Information). This discrepancy most likely arises from the fact that XRD probes the mean size of the coherently scattering domains, while TEM probes only pico- to nanograms of a sample and yields 2D projections of particles of unknown morphology.

On the contrary, XRD pattern analysis of the mixed sulfides yielded no meaningful results. Both the Williamson–Hall plot and full pattern refinement returned very small crystallite sizes (10–20 nm) and high strain values (Figures S8C,D and S9A, Supporting Information). The results were least realistic for the samples with the broadest diffraction lines: samples prepared in demineralized water and with the en-containing solution. Extended crystal defects (i.e., nanotwins, stacking faults, and dislocations) cannot explain these results, because the fraction of nanotwinned particles was always less than 10% (Table S4, Supporting Information). Moreover, high magnification TEM images indicate that the nontwinned particles are single crystals (Figure 6). Crystallite sizes consistent with the values estimated

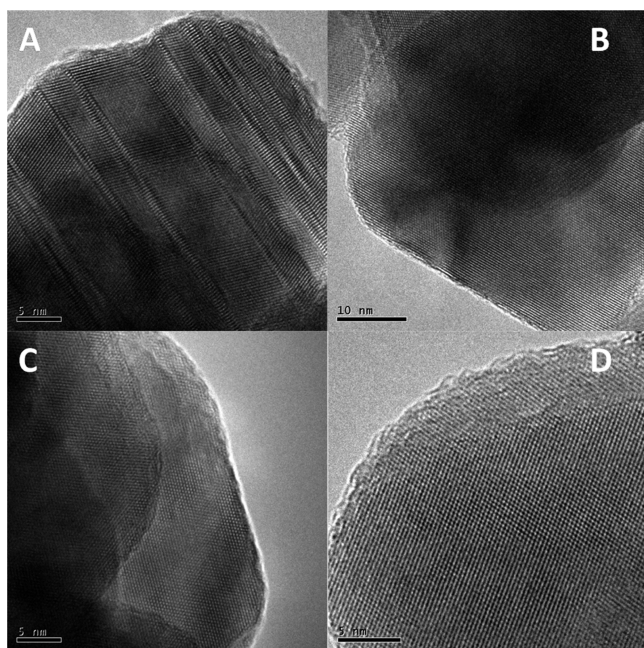


Figure 6. TEM images representing nanotwinned (A) and nontwinned (B–D) particles of Cd–Zn sulfides.

from TEM and microstrains close to the values obtained for pure ZnS and CdS were obtained from the full pattern refinement only when we assumed that a range of cubic crystal phases was present (Figure S9, Supporting Information). The lattice constants of these phases deviated from the value predicted for $\text{Cd}_{0.5}\text{Zn}_{0.5}\text{S}$ by Vegard's law.²⁸ In the model these phases represent Zn-rich, Cd-rich, and stoichiometric sulfides, and accordingly, we attribute the XRD line broadening to the compositional inhomogeneities of the mixed sulfide.²⁴

This interpretation helps to explain several observations. The presence of a Cd-rich phase can explain why samples with broader XRD lines exhibit smaller bandgaps (Figures 3 and 5).

This is consistent with the finding that the bandgap of mixtures of pure ZnS and CdS is strongly determined by the CdS component (Figure S11, Supporting Information). XRD lines of all mixed sulfides were significantly broader than those of ZnS or CdS, and the apparent bandgaps were smaller than the value predicted by Vegard's law for $\text{Cd}_{0.5}\text{Zn}_{0.5}\text{S}$ (≈ 3.0 eV). Thus, all samples exhibited compositional inhomogeneities in terms of the Zn/Cd ratio. This effect was more prominent for the samples prepared in en solutions or demineralized water. In contrast to XRD and UV–vis measurements that point to compositional heterogeneities, the bulk Zn/Cd ratio as determined by ICP–AES was similar for all samples. This implies that the Cd/Zn ratio varies on a particle basis, but the bulk composition is the same as to be expected since all Cd and Zn have been incorporated into the sulfides. The origin of these compositional inhomogeneities can be understood from the substantial differences in solubility products of Zn and Cd hydroxides and the corresponding sulfides (Table S3, Supporting Information). While Cd hydroxide is more soluble than Zn hydroxide, the reverse applies to the sulfides. This means that there will always be different driving forces for solubilization and precipitation of the hydroxides and sulfides of Zn and Cd, respectively. Accordingly, one expects the formation of particles with different Cd/Zn ratios at different stages of the synthesis as the amounts of hydroxides change. This is in keeping with the conclusions drawn from the XRD and UV–vis data. Thus, it is very difficult to obtain a truly homogeneous sample in terms of Cd/Zn distribution.

Influence of Nanotwinned Particles on Photocatalytic Activity. Liu et al. ascribed the enhanced photocatalytic activity of Cd–Zn sulfides prepared from the insoluble hydroxide to the presence of nanotwinned particles.¹⁰ Hence, a higher amount of such nanotwinned crystallites in a sample should result in higher photocatalytic activity. To check this hypothesis, we carried out a thorough TEM analysis of five Cd–Zn sulfide samples. The samples were divided into three groups based on their activity: (a) the least active sample (prepared in 1.0 M KCl), (b) a medium active sample (prepared in demineralized water) and (c) three most active samples (prepared in 1.0 M NaAc, 1.0 M NaPr, and 0.2 M en). We acquired at least 70 TEM images and analyzed more than 450 particles per sample (Table S4, Supporting Information). The results of this statistically sound analysis along with the activity of the samples are shown in Figure 7. As one can see, the least active sample had the largest fraction of the nanotwinned particles, while more active samples contained fewer. This shows that high photocatalytic activity cannot be linked to the occurrence of nanotwinned particles.¹⁰

We note that Liu et al. reported that the fraction of twinned particles in their samples was about 50%, which is five times higher than the highest amount observed in our study. Despite this difference, the activities of our samples are similar to the values reported by Liu et al., when the hydrogen production rates are normalized to the reference coprecipitated mixed sulfide (Table S5, Supporting Information). In addition to this, we observed that the freshly precipitated Cd–Zn hydroxide did not affect the nature of the resulting sulfide nor its performance (Figure S12, Supporting Information).

Liu et al. proposed that the nanotwinned particles have a built-in electrical potential that improves charge carrier separation and results in enhanced photocatalytic activity. First, we note that the particles which can be denoted “nanotwinned” contain stacking faults and dislocations along

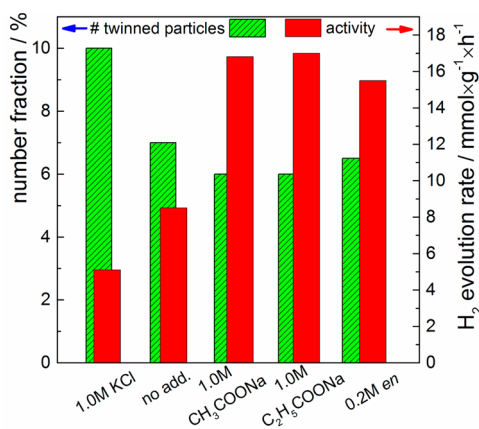


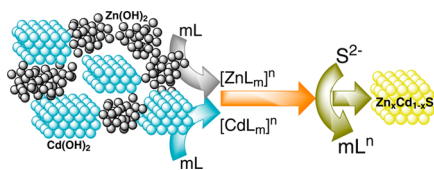
Figure 7. Number fraction of the twinned particles in Cd–Zn sulfides prepared in the presence of different additives and their photocatalytic activity.

with twin planes (Figure 6A). These extended defects are known to act as centers for nonradiative recombination of charge carriers.²⁹ Hence, a smaller number of nanotwinned particles in a sample may indicate that the synthesis condition favored formation of crystallites with fewer defects. This can explain the higher photocatalytic activity of samples with fewer nanotwinned particles as found in our study. Taking this into account, the deposition of Pt particles in between twin planes observed by Liu et al. can be a result of the fact that electrons can reach the surface of a particle only in the defect-free regions between twin planes, dislocations, or stacking faults.

We also evaluated the influence of platinization of the mixed sulfides. Although twinning is thought to enhance charge carrier separation, one can expect that not all of the photogenerated electrons will be involved in water reduction due to kinetic limitations. Adding Pt, a common and very efficient cocatalyst for the hydrogen evolution reaction, would then significantly increase the photocatalytic activity of samples containing more nanotwinned particles. The result in Figure S14 in the Supporting Information shows that the reverse holds: the sample prepared in 1.0 M KCl with more nanotwinned particles remains much less active after Pt photodeposition than the sample prepared in 1.0 M CH₃COONa. This adds further support to our conclusion that the photocatalytic activity of mixed Cd–Zn sulfides cannot be directly linked to nanotwinned particles.

Formation Mechanism of Mixed Cd–Zn Sulfides. On the basis of our findings, we sketch an overall mechanism of the formation of mixed Cd–Zn sulfides from a mixture of insoluble hydroxides (Scheme 1). This scheme is based on a dissolution–precipitation mechanism and not on direct ion exchange of OH[−] by S^{2−}.¹⁸ A direct ion exchange mechanism is unlikely to

Scheme 1. Dissolution–Precipitation Mechanism of the Formation of Mixed Cd–Zn Sulfide from the Mixed Hydroxide Precursor in Which L Represents a Ligand That Helps To Dissolve the Metal Hydroxides



take place in the investigated system for the following reasons: first, direct ion exchange would convert the mixture of amorphous Zn(OH)₂ and trigonal Cd(OH)₂ into ZnS and CdS, rather than into a solid solution. Second, one may expect at least partial preservation of the morphology of the precursor particles upon conversion into sulfides if direct ion exchange dominates. This is certainly not the case as can be seen from TEM (Figure S13, Supporting Information). Third, direct ion exchange cannot explain the influence of different additives on the activity.

In our mechanism, the insoluble hydroxides are first dissolved in the form of transition metal complexes. These complexes undergo ligand exchange for S^{2−} or thioacetamide and, eventually, precipitate in the form of sulfides (Scheme 1). We suppose that the formation of coordination compounds plays a central role in the conversion of the mixture of insoluble hydroxides into mixed sulfides; the exact way the mixed sulfides are formed will strongly affect their photocatalytic activity.

The influence of additives can be further understood by discussing literature data.^{30–32} Complexing agents are known to reduce nucleation rates and, in this way, to retard precipitation of sulfides.³⁰ This can lead to oversaturation and concomitant precipitation of both metals in the form of a solid solution. Inorganic salts influence the precipitation of CdS as well. For instance, sulfate was found to increase the rate of precipitation, whereas chloride extended the induction period.³¹ These effects can be discussed in terms of surface-diffusion controlled growth of crystallites.^{31,32} Thus, we surmise that additives adsorb on the facets of the growing crystallites and, depending on their nature, either hinder incorporation of new ions into the structure, which causes larger number of twin planes, dislocations, and stacking faults, or promote coherent growth of crystals with fewer defects (e.g., chloride and carboxylates respectively).

CONCLUSION

The influence of mechanical agitation and organic and inorganic additives on the photocatalytic activity of mixed Cd–Zn sulfide, prepared from the corresponding insoluble hydroxide, has been systematically studied. On the basis of the experimental results, we formulate a mechanism that describes the transformation of the hydroxide precursor, which was found to be a mixture of Zn(OH)₂ and Cd(OH)₂, into a Cd–Zn sulfide solid solution. The mechanism involves the dissolution of Zn and Cd hydroxides in the form of complexes, followed by ligand exchange and concomitant precipitation of the sulfides. Formation of the soluble intermediate complexes (e.g., hydroxo, diamino) is important for the formation of highly active photocatalysts. Mechanical agitation of the reaction medium during the hydrothermal synthesis suppresses the formation of the hexagonal phase of Cd–Zn sulfides; the cubic Cd–Zn sulfide phase shows better photocatalytic activity than the hexagonal phase does. The sample with the lowest photocatalytic activity contained the most nanotwinned particles. This trend can be understood in terms of the extended defects of the crystal structure (i.e., twins, stacking faults, and dislocations) and recombination of charge carrier at their boundaries. All samples of the mixed Cd–Zn sulfide displayed substantial compositional inhomogeneity which induced XRD line broadening and decrease of their apparent bandgaps due to the presence of Cd-rich phase.

■ ASSOCIATED CONTENT

■ Supporting Information

The Supporting Information is available free of charge on the ACS Publications website at DOI: 10.1021/acs.inorgchem.5b01396.

XRD patterns, photocatalytic tests results, XPS, UV–vis spectra, solubility products, and detailed data processing (PDF)

■ AUTHOR INFORMATION

Corresponding Author

*E-mail: e.j.m.hensen@tue.nl. Phone: +31 (0) 40-247 5178.

Author Contributions

The manuscript was written through contributions of all authors. All authors have given approval to the final version of the manuscript.

Notes

The authors declare no competing financial interest.

■ ACKNOWLEDGMENTS

The authors thank Dr. Tore Niermann (TU Berlin) for the fruitful discussions and Adelheid Elemans – Mehring for the ICP-AES analysis. This work is supported by NanoNextNL, a micro and nanotechnology consortium of the Government of The Netherlands and 130 partners: project NNNL.02B.08 CO2Fix-1.

■ REFERENCES

- (1) Elzinga, D.; Fulton, L.; Heinen, S.; Wasilik, O. *Advantage Energy: Emerging Economies, Developing Countries and the Private-Public Sector Interface*; OECD Publishing: Paris, 2011.
- (2) Kudo, A.; Miseki, Y. *Chem. Soc. Rev.* **2009**, *38*, 253–278.
- (3) Onsuratoom, S.; Chavadej, S.; Sreethawong, T. *Int. J. Hydrogen Energy* **2011**, *36*, 5246–5261.
- (4) Schneider, J.; Matsuoka, M.; Takeuchi, M.; Zhang, J.; Horiuchi, Y.; Anpo, M.; Bahnemann, D. W. *Chem. Rev.* **2014**, *114*, 9919–9986.
- (5) Yu, X.; An, X.; Shavel, A.; Ibanez, M.; Cabot, A. *J. Mater. Chem. A* **2014**, *2*, 12317–12322.
- (6) Biswal, N.; Parida, K. M. *Int. J. Hydrogen Energy* **2013**, *38*, 1267–1277.
- (7) Parida, K. M.; Biswal, N.; Das, D. P.; Martha, S. *Int. J. Hydrogen Energy* **2010**, *35*, 5262–5269.
- (8) Biswal, N.; Das, D. P.; Martha, S.; Parida, K. M. *Int. J. Hydrogen Energy* **2011**, *36*, 13452–13460.
- (9) Zhang, K.; Guo, L. *Catal. Sci. Technol.* **2013**, *3*, 1672–1690.
- (10) Liu, M.; Wang, L.; Lu, G.; Yao, X.; Guo, L. *Energy Environ. Sci.* **2011**, *4*, 1372–1378.
- (11) Yan, H.; Yang, J.; Ma, G.; Wu, G.; Zong, X.; Lei, Z.; Shi, J.; Li, C. *J. Catal.* **2009**, *266*, 165–168.
- (12) Liu, M.; Jing, D.; Zhou, Z.; Guo, L. *Nat. Commun.* **2013**, *4*, 2278.
- (13) Kominami, H.; Murakami, S.; Kera, Y.; Ohtani, B. *Catal. Lett.* **1998**, *56*, 125–129.
- (14) Murakami, S.-Y.; Kominami, H.; Kera, Y.; Ikeda, S.; Noguchi, H.; Uosaki, K.; Ohtani, B. *Res. Chem. Intermed.* **2007**, *33*, 285–296.
- (15) Yan, J.; Wu, G.; Guan, N.; Li, L.; Li, Z.; Cao, X. *Phys. Chem. Chem. Phys.* **2013**, *15*, 10978–10988.
- (16) Feitknecht, W.; Häberli, E. *Helv. Chim. Acta* **1950**, *33*, 922–936.
- (17) Yang, J.; Yan, H.; Wang, X.; Wen, F.; Wang, Z.; Fan, D.; Shi, J.; Li, C. *J. Catal.* **2012**, *290*, 151–157.
- (18) Bao, N.; Shen, L.; Takata, T.; Domen, K. *Chem. Mater.* **2008**, *20*, 110–117.
- (19) Wang, X.; Liu, G.; Chen, Z. G.; Li, F.; Lu, G. Q.; Cheng, H. M. *Electrochem. Commun.* **2009**, *11*, 1174–1178.

(20) Zhang, X.; Jing, D.; Liu, M.; Guo, L. *Catal. Commun.* **2008**, *9*, 1720–1724.

(21) Zhang, X.; Jing, D.; Guo, L. *Int. J. Hydrogen Energy* **2010**, *35*, 7051–7057.

(22) Dean, J. A. *Lange's Handbook Of Chemistry*, 15th ed.; McGraw-Hill: New York, 1999.

(23) Scherrer, P. *Nachr Ges Wiss Goettingen, Math-Phys. Kl.* **1918**, 98–100.

(24) Leineweber, A.; Mittemeijer, E. J. *Zeitschrift für Krist. Suppl.* **2006**, *1*, 117–122.

(25) Williamson, G. K.; Hall, W. H. *Acta Metall.* **1953**, *1*, 22–31.

(26) Estevez-Rams, E.; Penton Madrigal, A.; Scardi, P.; Leoni, M. *Zeitschrift für Krist. Suppl.* **2007**, *1*, 99–104.

(27) Rietveld, H. M. *J. Appl. Crystallogr.* **1969**, *2*, 65–71.

(28) Vegard, L. *Eur. Phys. J. A* **1921**, *5*, 17–26.

(29) Grundmann, M. *The Physics of Semiconductors: An Introduction Including Nanophysics and Applications*; Springer-Verlag: Berlin, 2010.

(30) Lewis, A. E. *Hydrometallurgy* **2010**, *104*, 222–234.

(31) Koumanakos, E.; Dalas, E.; Koutsoukos, P. G. *J. Chem. Soc., Faraday Trans.* **1990**, *86*, 973–977.

(32) Mullin, J. W. *Crystallization*, 3rd ed.; Butterworths Scientific Publications; Butterworth-Heinemann: Oxford, 1993.